RESEARCH

MRI-based analysis of the microstructure of the thalamus and hypothalamus and functional connectivity between cortical networks in episodic cluster headache

Chiara Abagnale[1,4*†], Antonio Di Renzo[2†], Giada Giuliani[3], Gabriele Sebastianelli[1], Francesco Casillo[1], Lucia Ziccardi[2], Vincenzo Parisi[2], Cherubino Di Lorenzo[1], Mariano Serrao[1], Francesca Caramia[3], Vittorio Di Piero[3] and Gianluca Coppola[1]

Abstract

Background Neuroimaging studies have shown that hypothalamic/thalamic nuclei and other distant brain regions belonging to complex cerebral networks are involved in cluster headache (CH). However, the exact relationship between these areas, which may be dependent or independent, remains to be understood. We investigated differences in resting-state functional connectivity (FC) between brain networks and its relationship with the microstructure of the hypothalamus and thalamus in patients with episodic CH outside attacks and healthy controls (HCs).

Methods We collected 3T MRI data from 26 patients with CH during the in-bout period outside the attacks and compared them with data from 20 HCs. From resting-state data we derived independent component (IC) networks. We calculated the fractional anisotropy (FA) and mean (MD), axial (AD), and radial (RD) diffusivity values of the hypothalamus and bilateral thalami and correlated them with resting-state IC Z-scores and CH clinical features.

Results Patients with CH had less FC between the salience network (SN) and left executive control network (ECN) than HCs, but more FC between the default mode network and right ECN. Patients with CH showed lower FA and higher MD microstructural hypothalamic metrics than HCs. Patients with CH had a higher bilateral FA metric in the thalamus than HCs. The AD and RD diffusivity metrics of the hypothalamus were positively correlated with the disease history duration. We found no correlations between the hypothalamic and thalamic diffusivity metrics and the FC of the cortical networks.

Conclusion Our findings presented the possibility of a correlation between the FC of the SN and the inability to switch between internalizing and externalizing brain activity during demanding cognitive tasks, such as

---

†Chiara Abagnale and Antonio Di Renzo contributed equally to this work.

*Correspondence:
Chiara Abagnale
chiara.abagnale@uniroma1.it

Full list of author information is available at the end of the article

recurring headaches. Moreover, we found differences in the thalamic and hypothalamic microstructures that may independently contribute to the pathophysiology of CH. These differences may reflect changes in directional organization, cell size, and density.

Keywords Cerebral networks, Diffusion, Salience, Executive, Default-mode, Hypothalamus, Thalamus

Introduction

Cluster headache (CH) attacks are characterized by severe stabbing pain along the sensory distribution territory of the trigeminal nerve and activation of the parasympathetic reflex, with the resulting autonomic manifestations ipsilateral to the side of the pain [1]. Comprehending the biology of CH might clarify misconceptions arising from the social and physical constraints imposed by the recurrent pain sickness [2]. Numerous clinical and experimental studies have emphasized the key role of the hypothalamus in the pathophysiology of CH [3]. Of the various nuclei that make up the hypothalamus, the suprachiasmatic nucleus located anteriorly (known as the master clock) is assumed to play a major role in this context, partially because of its connection to brainstem reticular formation and the trigeminal system [3]. Invasive deep inhibitory stimulation of the posterior hypothalamus can plastically reduce the recurrence of CH attacks, highlighting the possibility that more subregions of the hypothalamus may be involved [4]. However, several other brain areas outside the hypothalamus have been identified as sites of abnormality in CH in both structure and function [5].

In a whole-brain diffusion tensor imaging (DTI) 1.5T MRI study, compared with healthy participants, patients with in-bout episodic CH (eCH) under prophylactic medications, showed regionally higher absolute (radial and mean) diffusivities in the left medial frontal gyrus and sub-gyrus and lower absolute (axial, radial, and mean) diffusivities in the right parahippocampal gyrus of the limbic lobe, all areas previously involved in pain modulation [6]. Furthermore, the investigation employing probabilistic fiber tractography demonstrated the presence of highly consistent and direct anatomical connections between all regions exhibiting alterations in diffusivity indices and the ipsilateral hypothalamus [6]. In addition, another 1.5T MRI study showed that compared with healthy controls, the mean fractional anisotropy of the right amygdala, mean axial and mean diffusivity of the right caudate nucleus, and radial diffusivity of the right pallidum were higher in patients with CH; however, the mean anisotropy of the right pallidum was lower [7]. Nevertheless, none of these DTI investigations specifically focused their analyses on the hypothalamic region of interest while employing a more detailed 3T scan in medication-free patients.

In addition to structural MRI findings, multiple studies conducted on patients with eCH, both in- and out-of-bout, have revealed abnormal functional connectivity between the hypothalamus and various brain regions associated with the processing of salient information. These regions include the prefrontal cortex, anterior cingulate cortex, contralateral thalamus, ipsilateral basal ganglia, insula, and the cerebellar hemispheres [8–14]. These different and sometimes non-adjacent regions of the brain may work in coordination and form brain networks. Inside and outside cluster bout, a decreased resting-state functional coactivation was detected between the hypothalamus (ipsilateral and contralateral to the headache) and the salience network (SN) [12]. The authors interpret their results as due to a malfunctioning central pathway for pain modulation and dysregulation of the autonomic nervous system. A model to differentiate between CH and migraine found that the most significant MRI characteristics indicated crucial involvement of the thalamus. Specifically, patients with CH in the out of the bout phase exhibit reduced functional connectivity between the left thalamus and parietal brain regions, such as the precuneus and angular gyrus [15]. A more recent study showed reduced FC (functional connectivity) between bilateral thalamus and SN in patients with CH compared with healthy controls, regardless of the side of pain [16].

However, in most of the abovementioned studies, patients with eCH were receiving one or several prophylactic medications at the time of scanning, which may have altered the course of the disease and led to biased results. The aim of our study was to analyze hypothalamic and thalamic microstructures and simultaneously identify independent network abnormalities using functional MRI (fMRI) in patients with eCH who were not on prophylactic medications at the time of scanning during the bout outside the attacks. We use this multimodal approach because contemporary models of human brain organization demonstrate that anatomical architecture significantly impacts brain function, reflecting multisynaptic interactions within intricate large-scale multidimensional networks [17]. Consequently, functional brain features cannot be directly assessed from structural data but must be inferred by statistical models of various complexity, as employed in our study [18]. We have already utilized that approach in the investigation of migraine pathophysiology [19–24]. We hypothesized that the microstructural metrics of the thalamus and hypothalamus, along with the functional connectivity between cortical networks, may be concurrently altered during the

Abagnale *et al. The Journal of Headache and Pain*   (2025) 26:12

Page 3 of 10

bout, outside of attacks, and associated with the clinical features of eCH patients.

Methods

Participants

Twenty-six patients with eCH (ICHD III code 3.1.1 [1]) and strictly unilateral pain (15 of the right side) attending the Headache Centers of Rome (directed by Prof. Vittorio Di Piero) and Latina (directed by Prof. Gianluca Coppola) were recruited. Patients were scanned during the in-bouts period outside of the attacks. Other primary or secondary headache types were excluded by clinical and/or instrumental evaluation, as appropriate. We collected information on various patient clinical characteristics at the time of either the screening visit or the day of the scanning session, including daily attack frequency, mean severity of headache attacks (0–10), duration of the attacks (hours), and duration of history of eCH (years). The exclusion criteria were severe systemic or neurological/neuro-ophthalmological diseases or psychiatric disorders. Patients with eCH and a family history of migraine (1st -degree relatives) were also excluded. No preventive drugs were permitted during the 3 months preceding the observations in eCH. For comparison, 20 healthy controls (HCs) of comparable age and sex distributions were recruited from among medical students and healthcare professionals. They were devoid of any overt medical conditions, personal or family history of primary headaches or epilepsy, or regular drug intake.

None of the enrolled participants experienced sleep deprivation or alcohol ingestion on the day preceding the recordings. Caffeinated beverages were not allowed on the day of the recording. All the participants provided written informed consent to participate in the study, which was approved by the local ethics committee (N° 0295/2023). The study complied with the principles of the Declaration of Helsinki for Human Experimentation.

MRI data acquisition

MRI data were obtained using a Siemens 3T Verio scanner with a 12-channel head coil. Structural anatomic scans were performed using a T1-weighted sagittal magnetization-prepared rapid gradient echo (MPRAGE) series (TR: 1900 ms, TE: 2.93 ms, 176 sagittal slices, $0.508 \times 0.508 \times 1$ mm^3 voxels). We acquired an interleaved double-echo Turbo Spin Echo sequence proton density and T2-weighted images (repetition time: 3320ms, echo time: 10/103ms, matrix: 384×384, field of view: 220 mm, slice thickness: 4 mm, gap: 1.2 mm, 50 axial slices). fMRI data were obtained using T2*-weighted echoplanar imaging (TR, 3000 ms; TE, 30 ms; 40 axial slices, $3.906 \times 3.906 \times 3$ mm; 150 volumes). Functional resting scans lasted for 7 min and 30 s. During these sessions, the participants were instructed to relax, avoid motion,

and keep their eyes closed, but not fall asleep. Upon completion of the scanning, all participants indicated that they had not fallen asleep during the resting-state fMRI procedure.

DTI images were obtained with a single-shot echoplanar image sequence with the following parameters: repetition time (TR) = 12,200 ms, echo time (TE) = 94 ms, field of view (FOV) = 192 mm x 192 mm, matrix = 96×96, 2 mm x 2 mm in-plane resolution, slice thickness = 2 mm, 72 continuous axial slices with no gap, 1 volume anterior to posterior (AP) phase of encoding direction b = 0 s/mm^2, b = 1000 s/mm^2, and 30 diffusion directions were isotropically distributed on a sphere where one direction lacked diffusion weighting resulting in 31 volumes of the AP phase of encoding direction and 1 volume posterior to anterior (PA) phase of encoding direction b = 0.

fMRI preprocessing and data analysis

Data pre-processing was performed using SPM12 software (http://www.fil.ion.ucl.ac.uk/spm/) implemented in MATLAB (version R2016b, MathWorks, Inc., Natick, MA, USA). The data were realigned to the first volume to correct for head motion using a 6-parameter rigid body process and resliced using cubic spline interpolation. Moreover, in order to check motion, we calculated framewise displacement (FD), based on participants' root mean square values (RMS) [25], and their contrast was not statistically significant (HCs: 0.0323 ± 0.0374, CH patients: 0.0484 ± 0.0333, *p* = 0.86 unpaired 2-sample t-test).

Structural (T1–MPRAGE) and functional data were co-registered for each participant. All participant's f-MRI images were normalized by means of SPM12 default parameters (normalise est & wri functions). The normalization procedure transformed the structural and realigned EPI images into a standard stereotactic space based on Talairach and Tournoux [26], which was resampled 3 mm in each direction.

Finally, the normalized functional images were smoothed isotropically with a Gaussian kernel of 8 mm full width at half maximum.

Resting-state images were analyzed using spatial independent component analysis (ICA) with the infomax algorithm, which was implemented in the Group ICA of the fMRI Toolbox (GIFT- https://fsl.fmrib.ox.ac.uk/fsl) [27].

Two data reduction steps were performed using the principal component analysis (PCA): participant-specific and group-level steps.

First, the participant-specific data were reduced to 50 components and the participant-reduced data were concatenated across time. Secondly, at the group level, data were reduced to 20 group-independent components

(ICs) using the expectation-maximization algorithm included in GIFT [28].

Two separate group spatial ICAs were also performed in the HCs and patients to ensure that the resulting components had similar resting-state fluctuations in the two groups, that is the resulting components obtained from all 46 participants combined.

The number of ICs was estimated using the minimum description length (MDL) criterion [29]. Participant-specific spatial maps and time courses were obtained using the back-reconstruction approach (GICA) [30].

An expert neuroradiologist (F.C.) analyzed all group ICs identifying the RSNs [31, 32], omitting those located in the CSF, white matter, or with low correlation to gray matter because they can be artifacts, such as eye movements, head motion, or ballistic artifacts.

Indeed, we obtained eight functional networks: visuospatial (IC1), default mode network (DMN, IC3), executive control (ECN, IC5), salience (SN, IC7), ECN right and left (IC10 & IC12), DMN (IC16, ventral part), and medial visual (IC19) to be processed in the following step.

The Functional Network Toolbox (FNC; http://trendscenter.org/software/gift/) [27] was used to evaluate whether there were different correlations between the groups' networks (expressed as *CorrPosΔ*, i.e. the difference in correlation between groups of each networks' combination). It also shows the constrained maximal time-lagged (lag) correlation for every pair of component combinations.

Bandpass filter values were set between 0.033 Hz and 0.13 Hz.

DTI

Before pre-processing, all DTI volumes were visually inspected to screen for noisy artifacts due to cardiac pulsations, signal dropout, and motion artifacts.

Functional MRI of the Brain (FMRIB) Software Library (FSL version 6.0.6, https://fsl.fmrib.ox.ac.uk/fsl) was used to image data process [33–35].

Firstly, the b = 0 volumes AP and PA phase-encoding directions were used as references, and were processed by means of top-up tool to estimate [36] and correct [33] susceptibility-induced distortions.

The brain extraction tool (BET) creates brain masks from the topup's output b = 0 volumes [37].

Eddy tool corrected DTI volumes for susceptibility, eddy currents and subject movements, based on topup function output files, the brain mask created in the previous step and each input diffusion volume acquisition features.

Before the final step, the MRI-processed images were assessed using a quality control framework [38] to identify and possibly remove the bad quality dataset. In brief, quality control framework checked all participants' topup and eddy functions output files, distinguishing each dataset quality, finally identifying those need carefully visually inspection. At the time of scanning, it checked each dataset for artifacts. No artefactual DTI data were detected.

Lastly, the DTIFIT toolbox fits the preprocessed images based on a diffusion tensor model to yield the fractional anisotropy (FA), mean diffusivity (MD), axial diffusivity (AD), and radial diffusivity (RD), distortion-corrected DTI volumes, brain mask previously created, b values and vectors files as inputs.

Hypothalamus ROI [39] were defined by an expert neuroradiologist (F.C.) in MNI standard space using FSLeyes software (https://open.win.ox.ac.uk/pages/fsl/fsleyes/fsleyes/userdoc/index.html). Left and right thalamic ROIs were defined using FSLeyes atlases and inspected by the same neuroradiologist (F.C.) (Fig. 1). All ROIs were registered as MRI diffusion images using algorithms embedded in the FDT toolbox [40–43].

Statistical analysis

Group differences in demographic data were estimated using SPSS version 23 (IBM Corp., USA).

An unpaired 2-sample t-test was used to detect significant differences in the correlations and lag values between the independent components for controls and patients [27].

A p-value of 0.05 false discovery rate (FDR) corrected for multiple comparisons was considered significant.

The DTI characteristics were estimated based on previously defined ROIs for each group, and their values were compared using an unpaired 2-sample t-test.

An additional Holm-Bonferroni correction was performed to compensate for the number of ROIs; thus, the p-value was set to 0.01.

To search for correlations between DTI metrics, regional RS-fMRI network changes, and clinical features, the Z-max scores (voxel-wise analysis) of each IC network were extracted for each participant.

A p-value of 0.01 (0.05 / 4) was chosen to compensate for multiple comparisons due to the number of clinical variables.

Results

All the participants completed the recording sessions. Structural brain MRI revealed no white matter lesions.

Resting-state functional connectivity

We found a difference in FC between ICs encompassing interconnected areas of the SN (IC7) and left ECN (IC10), and in FC between ICs encompassing interconnected areas of the right ECN (IC12) and DMN (IC16) in patients with CH compared to HCs (Figs. 2 and 3). The difference between IC7-IC10 (corrPosΔ = 0.1994; $p = 0.0004$) was because of a lower positive significant
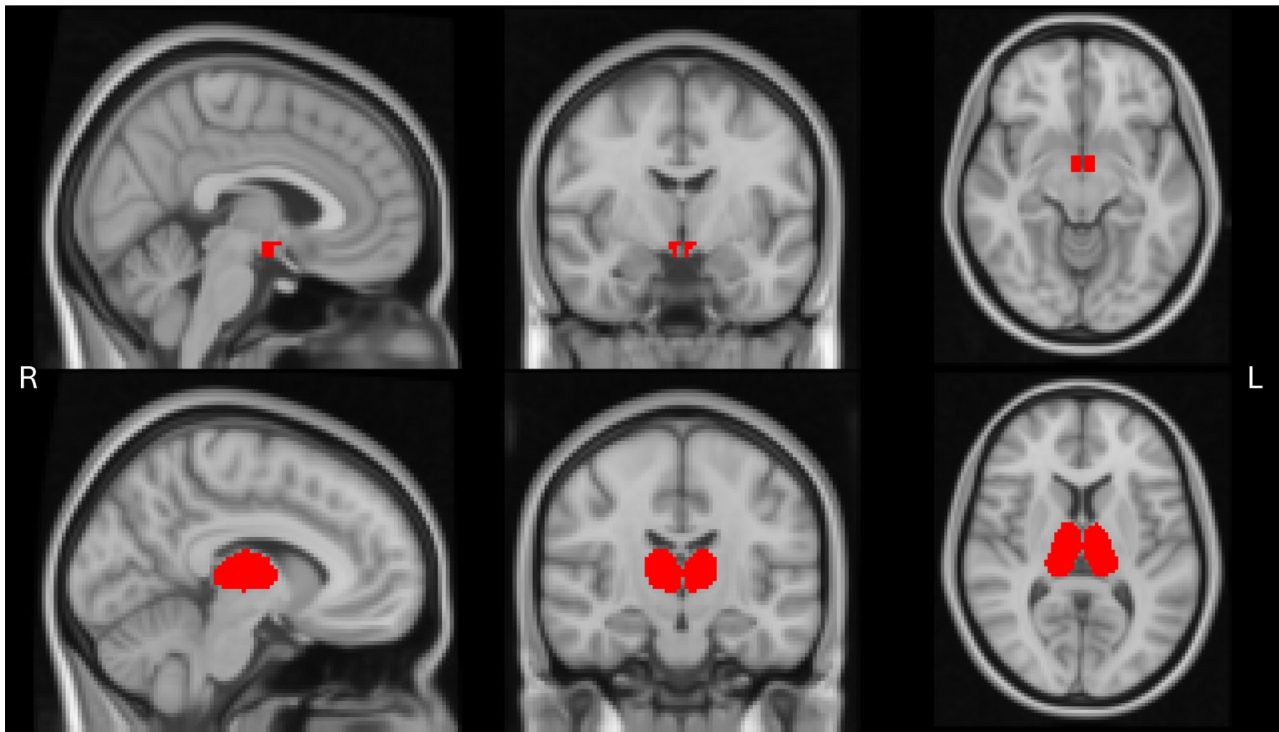
Fig. 1 Sagittal, coronal, and axial ROIs representations used to achieve DTI characteristics: hypothalamus and thalami highlighted in red
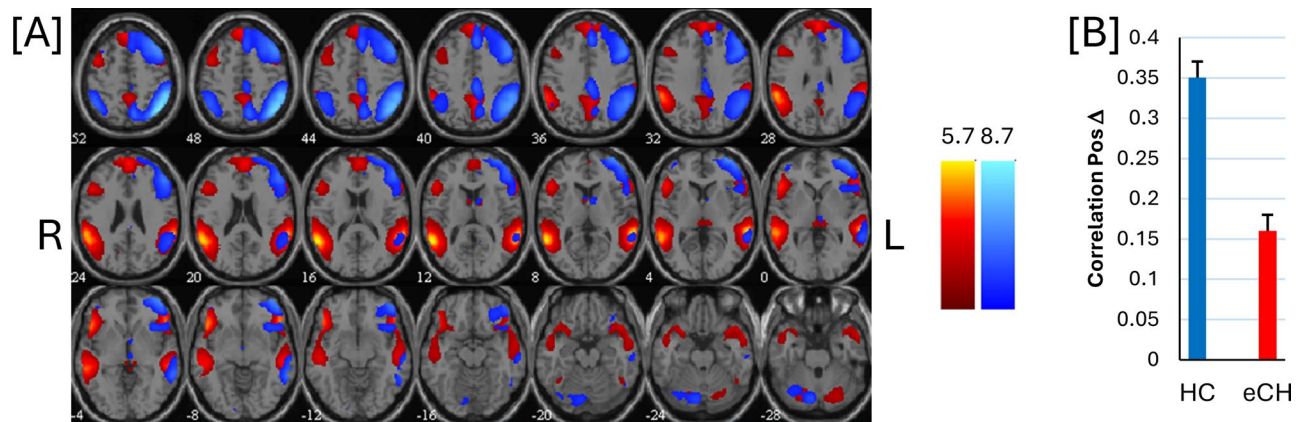
Fig. 2 Resting state functional connectivity between the salience network (IC7) and left executive control network (IC10). (**A**) A depiction of the two distinct components IC7 (hot metal scale) and IC10 (azure-blue) that were identified by independent component analysis (ICA). The functional connectivity absolute value of these components was found to be reduced in patients with episodic cluster headache (eCH) as compared to healthy controls (HC). The process of co-registration has been applied to align all images with the MNI template space. The numerals underneath each image indicate the z coordinate in Talairach's system. (**B**) The bar graph on the right shows the correlation between the 2 ICs in HC and eCH, at $p < 0.05$ FDR corrected

correlation between the IC pairs in patients with CH. In contrast, the difference between IC12-IC16 was because of significant negative CH connectivity and a lack of significant negative connectivity in HCs (corrPosΔ = -0.1880; $p = 0.0015$). No significant lag differences were detected between the contrasts listed above (See Table 1).

No additional significant differences were detected in the other ICs FC between eCHs and HCs.

Diffusion tensor imaging metrics

In patients with CH, the FA value of the hypothalamus was lower, and the MD was higher than in HCs ($p < 0.001$, Table 2). Additionally, the FA values of the bilateral thalami were higher in the CH group than in HC group ($p = 0.002$, Table 3).

Correlation analyses

There were no significant correlations between DTI metrics and the following clinical features of patients with
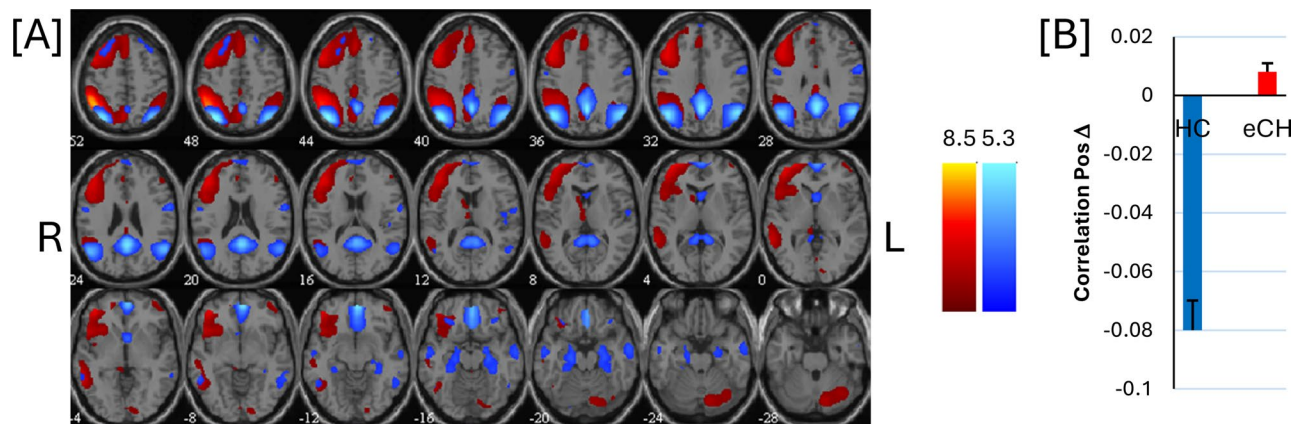
Fig. 3 Resting state functional connectivity between the right executive control network (IC12) and default-mode network (IC16). (**A**) A depiction of the two distinct components IC12 (hot metal scale) and IC16 (azure-blue) that were identified by independent component analysis (ICA). The functional connectivity absolute value of these components was found to be reduced in patients with episodic cluster headache (eCH) as compared to healthy controls (HC). The process of co-registration has been applied to align all images with the MNI template space. The numerals underneath each image indicate the z coordinate in Talairach's system. (**B**) The bar graph on the right shows the correlation between the 2 ICs in HC and eCH, at $p < 0.05$ FDR corrected

Table 1 Demographic and clinical characteristics (mean ± standard deviation) of the patients with episodic cluster headache (eCH) and of heathy control (HC) groups

	HC (*N* = 20)	eCH (*N* = 26)	Statistics
Age	40.2 ± 9.2	40.3 ± 10.3	t = − 0.007, *p* = 0.995
Sex (M/F)	(19/1)	(24/2)	Chi = 0.714, *p* = 0.599
Duration of history of eCH (years)		14.3 ± 10.96	
Mean severity of headache attacks (0–10)		9.69 ± 0.67	
Attacks frequency (N/day)		2.73 ± 2.01	
Attacks duration (mins)		85 ± 55.7	

Table 2 Diffusion tensor imaging (DTI) metrics of the hypothalamus of healthy controls (HC) and patients with episodic cluster headache (eCH). Data are expressed as means ± SD; * $p < 0.001$

DTI metrics	HC (*N* = 20)	eCH (*N* = 26)
Fractional anisotropy	0.410 ± 7.82E-2	0.223 ± 8.5E-2 *
Mean diffusivity	9.41E-4 ± 1.64E-4	1.949E-3 ± 6.26E-4 *
Axial diffusivity	1.27E-3 ± 1.61E-4	1.502E-3 ± 4.60E-4
Radial diffusivity	7.76E-4 ± 1.67E-4	1.027E-3 ± 4.37E-4

Table 3 Diffusion tensor imaging (DTI) metrics of bilateral thalami of healthy controls (HC) and in patients with episodic cluster headache (eCH). Data are expressed as means ± SD; * $p \leq 0.002$

DTI metrics	HC (*N* = 20)	eCH (*N* = 26)
Right		
Fractional anisotropy	0.327 ± 3.5E-2	0.361 ± 3.417E-2 *
Mean diffusivity	1.073E-3 ± 2.46E-4	1.060E-3 ± 1.74E-4
Axial diffusivity	1.383E-3 ± 2.59E-4	1.436E-3 ± 2.19E-4
Radial diffusivity	9.18E-4 ± 2.41E-4	9.39E-4 ± 2.00E-4
Left		
Fractional anisotropy	0.335 ± 2.49E-2	0.366 ± 3.89E-2 *
Mean diffusivity	9.78E-4 ± 1.72E-4	1.040E-3 ± 1.59E-4
Axial diffusivity	1.28E-3 ± 1.90E-4	1.376E-3 ± 2.07E-4
Radial diffusivity	8.27E-4 ± 1.64E-4	8.83E-4 ± 1.72E-4

CH: daily attack frequency, mean severity of headache attacks, and duration of attacks. The only correlation we found was that the higher the AD ($R^2 = 27.84\%$, $p = 0.009$) and RD ($R^2 = 30.50\%$, $p = 0.005$) of the hypothalamus in CH patients, the longer the history of the disease.

There were no correlations between ICs Z-score and DTI parameters.

Discussion

In the present study, we searched for structural and functional MRI abnormalities in patients with eCH who were not receiving prophylactic medication at the time of scanning. The key results of this DTI-fMRI study are summarized as follows:

a) Compared to HCs, the functional connectivity between the salience network and the left executive control network was reduced in patients with CH.
b) The right executive control and default mode network were positively connected in patients and negatively connected in HCs.
c) The FA value of the hypothalamus was significantly lower and the MD value was significantly higher in patients with CH than in HCs.

d) The FA values of the bilateral thalami were higher in patients with CH than in HCs.

e) A longer disease history was associated with higher AD and RD metrics in the hypothalamus.

Microstructural alterations

Using 1.5T DTI and tract-based spatial statistics, significant differences in white matter diffusivity metrics (axial, radial, and mean) were found in the parahippocampal gyrus, amygdala, insula, frontal subgyral area, extranuclear area of the putamen, and medial frontal gyrus areas consistently during the in-bout and out-of-bout periods in 17 patients with CH compared with HCs [6]. The ipsilateral hypothalamus was highly connected to the ipsilateral medial frontal gyrus and the contralateral parahippocampal gyrus [6]. Analysis of whole-head 1.5T MRI DTI in tract-based spatial statistics in a variable number of patients (from 7 to 22) revealed diffuse white matter microstructure plastic changes in patients with CH [7, 44, 45]. In seven male patients with episodic CH, significant microstructural white matter tissue changes were detected in the brainstem; frontal, temporal, and occipital lobes; internal capsule; and right thalamus and cerebellum bilaterally [44]. This widespread involvement of the white matter regions in CH was confirmed by Szabo et al., who found higher mean, axial, and perpendicular diffusivity in the frontal, parietal, temporal, and occipital lobes; lower FA in the corpus callosum; and some frontal and parietal white matter tracts mainly contralateral to the pain [45]. The mean FA of the right amygdala, mean AD and MD of the right caudate nucleus, and RD of the right pallidum were higher, and the mean FA of the right pallidum was lower in a DTI study in patients with CH than in HC [7]. None of the previous studies have included the hypothalamic ROI in their analysis. Here, we found a lower FA value and a higher MD value in the hypothalamus of patients with CH than in HCs. These altered values can support the hypothesis that the hypothalamus plays a role in the pathogenesis of CH. Within white matter, diffusion is more likely to occur in a direction that aligns with the orientation of the fibers. This emphasizes that the main factors contributing to an increase in FA are a decrease in RD and/or an increase in AD [46]. This DTI technique is valuable for identifying both large brain white matter pathways and white matter tracts within gray matter nuclei, such as the hypothalamus and thalamus [47]. These brain structures consist of separate nuclei bound together by highly anisotropic myelinated fibers [48].

Nevertheless, it must be pointed out that myelin accounts for merely 20% of anisotropy, as variations in the volume of the axonal membrane and changes in the structure of glial cells appear to be additional factors in the development of MD and FA, respectively [46, 49].

Furthermore, in the gray matter, the primary factors contributing to FA are the abundance of neuronal connections through the branching and crossing of dendritic trees, number of local circuits, and abundance of axonal membranes [49]. Therefore, the present diffusivity pattern of decreased FA and increased MD compared with those of HCs may reflect the loss of preferential direction of the fibers in combination with increased cell swelling. From a neurophysiological perspective, this pattern may coincide with an increased neuronal electrical response with a consequent increase in neuronal connections and dendritic arborization, resulting in an increased number of local circuits [49, 50]. Interestingly, a longer history of the disease was associated with higher AD and RD values in the hypothalamus. However, as both metrics in the eCH group were within normal limits, we hypothesized that disease history may only marginally influence microstructural changes in the hypothalamus.

Contrary to what we found in the hypothalamus, the FA of the bilateral thalami increased in the presence of normal MD, AD, and RD in the patients compared to HCs. From a microstructural perspective, these findings may indicate an increase in the directional arrangement while maintaining the same neuronal and glial cell size and density. Based on these results, we argue that the thalamus also plays a role in CH pathophysiology, regardless of the side of pain. Given the thalamus's established role in both descending and ascending trigeminal pain processing and autonomic system regulation, we can only speculate that the increased directionality of the thalamic fibers may result from recurrent headaches amplifying pain transmission in our patients with eCH. The recent finding in a cohort of eCH of diminished thalamic-to-SN FC irrespective of headache lateralization, may corroborate our hypothesis, as an anomalous involvement of the thalamus in pain processing could impair saliency detection mechanisms in the brain [16], specifically its ability to switch between systems engaged in processing exogenous and self-relevant information [51]. Further studies of functional connectivity are required to elucidate this point.

Between networks connectivity

Previous investigations using resting-state functional MRI have identified intrinsic changes in the connectivity of brain networks in individuals with CH. Patients have FC alterations in various brain networks, including the temporal, frontal, salience, default mode, sensorimotor, dorsal attention, and visual networks, regardless of whether they were in or out of the bouts [52]. Decreased functional coactivation between the hypothalamus ipsilateral and contralateral to the headache side and the SN indicated that dysfunction in the hypothalamus on the same side as the headache is insufficient to explain

all abnormalities associated with CH [12]. A combined voxel-based morphometry and functional MRI study showed that in patients with CH, compared to migraine without aura patients and HCs, decreased regional grey matter volume in the frontal cortex and higher FC in the prefrontal cortex, brain area belonging to the ECN, and in the DMN were observed [53].

In humans, the SN detects and filters salient environmental stimuli and regulates attention and behavior in connection with the neurolimbic system. In healthy individuals, the SN switches between the DMN, which is active when the brain is at rest and not focused on the outside world, and the ECN, a task-oriented brain network, during goal-directed tasks [54, 55]. The SN, which includes the dorsal anterior cingulate cortex and bilateral anterior insula/frontal operculum, may be essential for emotions, pain, and interoception. The ACC of the SN has a vital role in affective and attentional modulation of pain perception, as well as in antinociception. Analysis of extensive brain networks led to the hypothesis that these three principal networks (SN, ECN, and DMN) constitute the ultimate common channel through which various internal or environmental disturbances may affect the brain [56]. Deviant connections within and among these brain networks have been shown to promote the onset of neuropsychiatric disorders [57] and have been further applied to elucidate the chronicity of pain [58]. By exploring between independent networks connectivity, we found reduced FC between the SN and left ECN and the presence of an unphysiological co-activation and increased FC between the DMN and right ECN in patients compared with HCs. Based on prior results acquired from healthy individuals, our findings in patients with CH may be a functional correlate of the patients' SN being unable to switch between the DMN and ECN during demanding cognitive tasks, such as integration of attentional, sensory and affective problems related to recurring headaches. These problems may contribute significantly to morbidity, resulting in heightened functional disability and diminished quality of life. Additional research is required to confirm whether this connectivity pattern is a physiological mechanism by which the brain attempts to cognitively modify the perceptions and neural responses triggered by the sensation of pain [59]. Typically, this neurological process includes increased natural pain-relieving activity in the descending pain-modulatory system (such as the prefrontal cortex belonging to the ECN) and reduced activity in regions that contribute to pain [60].

Limitations

Our study has several limitations. First, cross-sectional fMRI studies with a relatively small cohort of subjects restrict their ability to draw conclusions regarding causality. Furthermore, as all patients were in the bout at the time of scanning, the data did not offer any insight into the brain processes during the period of remission. However, disturbances in the connectivity of large-scale brain networks have consistently been detected both in and out of bouts in individuals with eCH. Second, a limitation of the current analysis is its failure to account for headache laterality, given that CH is characterized by strictly unilateral pain. Third, this a cross-sectional study on a relatively small cohort of subjects and with retrospective collection of clinical data. Further research employing the same techniques in a larger cohort of subjects is required to control for the laterality of pain, track patients over time, and investigate individuals with chronic CH, where a more significant impact on the midbrain has been suggested [3].

Conclusions

In our study, we emphasized how the hypothalamic microstructure is altered during the in-bout period outside of attacks. We also highlighted the presence of altered bilateral thalamic metric values and demonstrated the role of the thalamus in the pathogenesis of CH attacks. In addition, we demonstrated that altered connectivity in networks that differentiate between patients with CH and HCs may be related to the SN and not the switching ability between internalizing the DMN and externalizing the ECN during pain. Further studies are needed to determine whether these functional abnormalities are related to the constant activity of the hypothalamus or to stable, genetically determined, disease-predisposing anomalies.

Abbreviations
AD	axial diffusion
CH	cluster headache
DMN	default-mode network
DTI	diffusion tensor imaging
eCH	episodic cluster headache
ECN	executive control network
FA	fractional anisotropy
FC	functional connectivity
FDR	false discovery rate
fMRI	functional magnetic resonance imaging
HC	healthy control
IC	independent component
MD	mean diffusion
RD	radial diffusion
SN	salience network

Declarations

Ethics approval and consent to participate
All the participants provided written informed consent to participate in the study, which was approved by the local ethics committee (N° 0295/2023).

Consent for publication
Not applicable.

Competing interests
The authors declare no competing interests.

Author details
[1]Department of Medico-Surgical Sciences and Biotechnologies, Sapienza University of Rome Polo Pontino, Latina, Italy
[2]IRCCS – Fondazione Bietti, Rome, Italy
[3]Department of Human Neurosciences, Sapienza University of Rome, Rome, Italy
[4]Department of Medico-Surgical Sciences and Biotechnologies, Sapienza University of Rome Polo Pontino - ICOT, Via Franco Faggiana 1668, Latina 04100, Italy

References

1. (2018) Headache Classification Committee of the International Headache Society (IHS) The International Classification of Headache Disorders, 3rd edition. Cephalalgia 38:1–211. https://doi.org/10.1177/0333102417738202
2. Pohl H, Gantenbein AR, Sandor PS et al (2022) Cluster headache and the Comprehension Paradox. SN Compr Clin Med 4:32. https://doi.org/10.1007/s42399-021-01083-z
3. Coppola G, Abagnale C, Sebastianelli G, Goadsby PJ (2024) Pathophysiology of cluster headache: from the trigeminovascular system to the cerebral networks. Cephalalgia Int J Headache 44:3331024231209317. https://doi.org/10.1177/03331024231209317
4. Leone M, Franzini A, Broggi G, Bussone G (2003) Hypothalamic deep brain stimulation for intractable chronic cluster headache: a 3-year follow-up. Neurol Sci off J Ital Neurol Soc Ital Soc Clin Neurophysiol 24(Suppl 2):S143–S145. https://doi.org/10.1007/s100720300063
5. Iacovelli E, Coppola G, Tinelli E et al (2012) Neuroimaging in cluster headache and other trigeminal autonomic cephalalgias. J Headache Pain 13:11–20. https://doi.org/10.1007/s10194-011-0403-8
6. Chou K-H, Yang F-C, Fuh J-L et al (2014) Altered white matter microstructural connectivity in cluster headaches: a longitudinal diffusion tensor imaging study. Cephalalgia Int J Headache 34:1040–1052. https://doi.org/10.1177/0333102414527649
7. Király A, Szabó N, Párdutz Á et al (2018) Macro- and microstructural alterations of the subcortical structures in episodic cluster headache. Cephalalgia Int J Headache 38:662–673. https://doi.org/10.1177/0333102417703762
8. Morelli N, Pesaresi I, Cafforio G et al (2009) Functional magnetic resonance imaging in episodic cluster headache. J Headache Pain 10:11–14. https://doi.org/10.1007/s10194-008-0085-z
9. Rocca MA, Valsasina P, Absinta M et al (2010) Central nervous system dysregulation extends beyond the pain-matrix network in cluster headache. Cephalalgia Int J Headache 30:1383–1391. https://doi.org/10.1177/0333102410365164
10. Qiu E, Wang Y, Ma L et al (2013) Abnormal brain functional connectivity of the hypothalamus in cluster headaches. PLoS ONE 8:e57896. https://doi.org/10.1371/journal.pone.0057896
11. Yang F-C, Chou K-H, Fuh J-L et al (2015) Altered hypothalamic functional connectivity in cluster headache: a longitudinal resting-state functional MRI study. J Neurol Neurosurg Psychiatry 86:437–445. https://doi.org/10.1136/jnnp-2014-308122
12. Qiu E, Tian L, Wang Y et al (2015) Abnormal coactivation of the hypothalamus and salience network in patients with cluster headache. Neurology 84:1402–1408. https://doi.org/10.1212/WNL.0000000000001442
13. Faragó P, Szabó N, Tóth E et al (2017) Ipsilateral alteration of resting state activity suggests that cortical dysfunction contributes to the pathogenesis of Cluster Headache. Brain Topogr 30:281–289. https://doi.org/10.1007/s10548-016-0535-x
14. Chen Y, Xing X, Dai W et al (2022) Brain regions involved in fractional amplitude of low-frequency fluctuation in cluster headache patients: a resting-state functional MRI study. BMC Neurol 22:336. https://doi.org/10.1186/s12883-022-02863-3
15. Messina R, Sudre CH, Wei DY et al (2023) Biomarkers of Migraine and Cluster Headache: differences and similarities. Ann Neurol 93:729–742. https://doi.org/10.1002/ana.26583
16. Qiu E, Xing X, Wang Y, Tian L (2024) Altered functional connectivity of the thalamus and salience network in patients with cluster headache: a pilot study. Neurol Sci off J Ital Neurol Soc Ital Soc Clin Neurophysiol 45:269–276. https://doi.org/10.1007/s10072-023-07011-4
17. Suárez LE, Markello RD, Betzel RF, Misic B (2020) Linking structure and function in Macroscale Brain Networks. Trends Cogn Sci 24:302–315. https://doi.org/10.1016/j.tics.2020.01.008
18. Tozzi A (2019) The multidimensional brain. Phys Life Rev 31:86–103. https://doi.org/10.1016/j.plrev.2018.12.004
19. Coppola G, Di Renzo A, Tinelli E et al (2016) Thalamo-cortical network activity between migraine attacks: insights from MRI-based microstructural and functional resting-state network correlation analysis. J Headache Pain 17:100. https://doi.org/10.1186/s10194-016-0693-y
20. Coppola G, Di Renzo A, Tinelli E et al (2016) Thalamo-cortical network activity during spontaneous migraine attacks. Neurology 87:2154–2160. https://doi.org/10.1212/WNL.0000000000003327
21. Coppola G, Di Renzo A, Tinelli E et al (2021) Thalamo-cortical networks in subtypes of migraine with aura patients. J Headache Pain 22:58. https://doi.org/10.1186/s10194-021-01272-0
22. Porcaro C, Di Renzo A, Tinelli E et al (2020) Haemodynamic activity characterization of resting state networks by fractal analysis and thalamocortical morphofunctional integrity in chronic migraine. J Headache Pain 21:112. https://doi.org/10.1186/s10194-020-01181-8
23. Porcaro C, Di Renzo A, Tinelli E et al (2021) Hypothalamic structural integrity and temporal complexity of cortical information processing at rest in migraine without aura patients between attacks. Sci Rep 11:1–11. https://doi.org/10.1038/s41598-021-98213-3
24. Porcaro C, Di Renzo A, Tinelli E et al (2022) A hypothalamic mechanism regulates the duration of a migraine attack: insights from Microstructural and temporal complexity of cortical functional networks analysis. Int J Mol Sci 23:13238. https://doi.org/10.3390/ijms232113238
25. Power JD, Barnes KA, Snyder AZ et al (2012) Spurious but systematic correlations in functional connectivity MRI networks arise from subject motion. NeuroImage 59:2142–2154. https://doi.org/10.1016/j.neuroimage.2011.10.018
26. Dervin J (1990) Co-planar Stereotaxic Atlas of the human brain 3-Dimensional Proportional System: an Approach to Cerebral Imaging 1988. J Talairich P Tournoux Mark Rayport Georg Thieme Verlag Stuttgart New York 3(13):711–701. 1 Price DM 268. pp. 122. Illustrations 130. J Laryngol Otol 104:72–72. https://doi.org/10.1017/S0022215100111879.
27. Jafri M, Pearlson GD, Stevens M, Calhoun VD (2008) A method for functional network connectivity among spatially independent resting-state components in schizophrenia. NeuroImage 39:1666–1681
28. Allen EA, Damaraju E, Plis SM et al (2014) Tracking whole-brain connectivity dynamics in the resting state. Cereb Cortex N Y N 1991 24:663–676. https://doi.org/10.1093/cercor/bhs352
29. Calhoun VD, Adali T, Pearlson GD, Pekar JJ (2001) A method for making group inferences from functional MRI data using independent component analysis. Hum Brain Mapp 14:140–151. https://doi.org/10.1002/hbm.1048
30. Calhoun VD, Adali T, Pearlson GD, Pekar JJ (2001) Spatial and temporal independent component analysis of functional MRI data containing a pair of

task-related waveforms. Hum Brain Mapp 13:43–53. https://doi.org/10.1002/hbm.1024

31. Griffanti L, Douaud G, Bijsterbosch J et al (2017) Hand classification of fMRI ICA noise components. NeuroImage 154:188–205. https://doi.org/10.1016/j.neuroimage.2016.12.036

32. Beckmann CF, DeLuca M, Devlin JT, Smith SM (2005) Investigations into resting-state connectivity using independent component analysis. Philos Trans R Soc Lond B Biol Sci 360:1001–1013. https://doi.org/10.1098/rstb.2005.1634

33. Smith SM, Jenkinson M, Woolrich MW et al (2004) Advances in functional and structural MR image analysis and implementation as FSL. NeuroImage 23 Suppl 1S208–219. https://doi.org/10.1016/j.neuroimage.2004.07.051

34. Woolrich MW, Jbabdi S, Patenaude B et al (2009) Bayesian analysis of neuroimaging data in FSL. NeuroImage 45:S173–186. https://doi.org/10.1016/j.neuroimage.2008.10.055

35. Jenkinson M, Beckmann CF, Behrens TEJ et al (2012) FSL NeuroImage 62:782–790. https://doi.org/10.1016/j.neuroimage.2011.09.015

36. Andersson JLR, Skare S, Ashburner J (2003) How to correct susceptibility distortions in spin-echo echo-planar images: application to diffusion tensor imaging. NeuroImage 20:870–888. https://doi.org/10.1016/S1053-8119(03)00336-7

37. Smith SM (2002) Fast robust automated brain extraction. Hum Brain Mapp 17:143–155. https://doi.org/10.1002/hbm.10062

38. Bastiani M, Cottaar M, Fitzgibbon SP et al (2019) Automated quality control for within and between studies diffusion MRI data using a non-parametric framework for movement and distortion correction. NeuroImage 184:801–812. https://doi.org/10.1016/j.neuroimage.2018.09.073

39. Baroncini M, Jissendi P, Balland E et al (2012) MRI atlas of the human hypothalamus. NeuroImage 59:168–180. https://doi.org/10.1016/j.neuroimage.2011.07.013

40. Jenkinson M, Smith S (2001) A global optimisation method for robust affine registration of brain images. Med Image Anal 5:143–156. https://doi.org/10.1016/s1361-8415(01)00036-6

41. Jenkinson M, Bannister P, Brady M, Smith S (2002) Improved optimization for the robust and accurate linear registration and motion correction of brain images. NeuroImage 17:825–841. https://doi.org/10.1016/s1053-8119(02)91132-8

42. Greve DN, Fischl B (2009) Accurate and robust brain image alignment using boundary-based registration. NeuroImage 48:63–72. https://doi.org/10.1016/j.neuroimage.2009.06.060

43. Non-linear registration aka spatial normalisation FMRIB Technial report TR07JA2 – ScienceOpen. https://www.scienceopen.com/book?vid=13f3b9a9-6e99-4ae7-bea2-c1bf0af8ca6e. Accessed 1 Nov 2024

44. Teepker M, Menzler K, Belke M et al (2012) Diffusion tensor imaging in episodic cluster headache. Headache 52:274–282. https://doi.org/10.1111/j.1526-4610.2011.02000.x

45. Szabó N, Kincses ZT, Párdutz Á et al (2013) White matter disintegration in cluster headache. J Headache Pain 14:64. https://doi.org/10.1186/1129-2377-14-64

46. Alexander AL, Lee JE, Lazar M, Field AS (2007) Diffusion tensor imaging of the brain. Neurother J Am Soc Exp Neurother 4:316–329. https://doi.org/10.1016/j.nurt.2007.05.011

47. Sedrak M, Gorgulho A, Frew A et al (2011) Diffusion tensor imaging and colored fractional anisotropy mapping of the ventralis intermedius nucleus of the thalamus. Neurosurgery 69:1124–1129 discussion 1129–1130. https://doi.org/10.1227/NEU.0b013e3182296a42

48. Mang SC, Busza A, Reiterer S et al (2012) Thalamus segmentation based on the local diffusion direction: a group study. Magn Reson Med 67:118–126. https://doi.org/10.1002/mrm.22996

49. Beaulieu C (2002) The basis of anisotropic water diffusion in the nervous system - a technical review. NMR Biomed 15:435–455. https://doi.org/10.1002/nbm.782

50. Tasaki I, Byrne PM (1992) Rapid structural changes in nerve fibers evoked by electric current pulses. Biochem Biophys Res Commun 188:559–564. https://doi.org/10.1016/0006-291x(92)91092-5

51. Menon V (2015) Salience Network. In: Toga AW (ed) Brain mapping. Academic: Elsevier, pp 597–611

52. Chou K-H, Yang F-C, Fuh J-L et al (2017) Bout-associated intrinsic functional network changes in cluster headache: a longitudinal resting-state functional MRI study. Cephalalgia Int J Headache 37:1152–1163. https://doi.org/10.1177/0333102416668657

53. Giorgio A, Lupi C, Zhang J et al (2020) Changes in grey matter volume and functional connectivity in cluster headache versus migraine. Brain Imaging Behav 14:496–504. https://doi.org/10.1007/s11682-019-00046-2

54. Seeley WW, Menon V, Schatzberg AF et al (2007) Dissociable intrinsic connectivity networks for salience processing and executive control. J Neurosci off J Soc Neurosci 27:2349–2356. https://doi.org/10.1523/JNEUROSCI.5587-06.2007

55. Menon V, Uddin LQ (2010) Saliency, switching, attention and control: a network model of insula function. Brain Struct Funct 214:655–667. https://doi.org/10.1007/s00429-010-0262-0

56. Menon V (2011) Large-scale brain networks and psychopathology: a unifying triple network model. Trends Cogn Sci 15:483–506. https://doi.org/10.1016/j.tics.2011.08.003

57. Menon B (2019) Towards a new model of understanding – the triple network, psychopathology and the structure of the mind. Med Hypotheses 133:109385. https://doi.org/10.1016/j.mehy.2019.109385

58. De Ridder D, Vanneste S, Smith M, Adhia D (2022) Pain and the Triple Network Model. Front Neurol 13. https://doi.org/10.3389/fneur.2022.757241

59. Kucyi A, Salomons TV, Davis KD (2013) Mind wandering away from pain dynamically engages antinociceptive and default mode brain networks. Proc Natl Acad Sci U S A 110:18692–18697. https://doi.org/10.1073/pnas.1312902110

60. Wiech K, Ploner M, Tracey I (2008) Neurocognitive aspects of pain perception. Trends Cogn Sci 12:306–313. https://doi.org/10.1016/j.tics.2008.05.005

Publisher's note